The Astrophysical Journal, 658:480–486, 2007 March 20


# THE LUPUS ASSOCIATION OF PRE–MAIN-SEQUENCE STARS: CLUES TO STAR FORMATION SCATTERED IN SPACE AND TIME

Valeri V. Makarov
Michelson Science Center, California Technology Institute, Pasadena, CA; vvm@caltech.edu
*Received 2006 September 20; accepted 2006 November 28*

## ABSTRACT

Kinematical analysis of spectroscopically identified pre–main-sequence stars associated with the Lupus dark cloud reveals a streamlike motion of low internal velocity dispersion ($\leq$1.3 km s$^{-1}$). A statistically significant mismatch between the convergent point radial velocity and the spectroscopic radial velocity from the literature indicates a moderate degree of expansion. The rate of expansion is too low to account for the present extent of the association if one assumes that the spatially dispersed population was formed in the dense molecular cores observed today. Therefore, it is unlikely that the outlying weak-lined T Tauri members were born in the same star-forming cores as the more compactly located classical T Tauri stars, despite the kinematic integrity of the association. Distances inferred from the classical moving-cluster method show a large depth of the association ($\sim$80 pc) along the line of sight. A color-magnitude diagram of the association in the near-IR colors corrected for the distribution of distances shows a clear gap separating the older (5–27 Myr) and the younger ($\sim$1 Myr) generations of stars. Half of the identified 1 Myr old stars lie in the tight group of mostly classical T Tauri stars associated with the Lupus 3 dark filament. This nest of very young stars appears to be 25 pc farther from the Sun than the center of the greater Lupus association.

*Subject headings:* open clusters and associations: individual (Lupus) — stars: distances — stars: formation — stars: kinematics — stars: pre–main-sequence

## 1. INTRODUCTION

The Lupus cloud complex is one of the nearest star formation regions that were not so long ago found to be surrounded by extended associations of T Tauri stars. The origin of these dispersed groups is an open issue. They appear to include classical T Tauri stars (CTTSs), as well as weak-lined T Tauri stars (WTTSs), of mixed ages and levels of X-ray and chromospheric activity. Age determination from evolution tracks is complicated by the significant and nonuniform extinction in the shredded clouds. In Lupus, evidence was found that CTTS members are closer in celestial projection to the denser cores of the cloud than their WTTS counterparts, and remote members are on average older than those closer to the cores (Wichmann et al. 1997). This appears to support the much discussed supposition that dense cores can be stable over extended time spans (>10 Myr), continuously generating new stars, which drift away because of the intrinsic velocity dispersion.

However, no observational evidence has been presented that the dispersed WTTS members of the Lupus association emerged from the same dense cores we observe today. The youngest stars in Lupus tend to huddle close to these cores, so their origin is fairly certain. But the older, strongly dispersed WTTS population could be formed in a different core or in multiple separated cores at some earlier times, which have dissipated or blended with the surrounding areas. This is the model of dynamical star formation in situ (Hartmann et al. 2001), as opposed to the standard scenario based on ambipolar diffusion of a magnetic field (Shu et al. 1987; Mouschovias et al. 2006 and references therein), which requires stable, long-lived ($\gtrsim$10 Myr) molecular cores. The maximum extent of the Lupus association on the sky is up to 40 pc (assuming a median distance of 145 pc). If not less than half of the Lupus members are younger than 6 Myr (Wichmann et al. 1997), the standard stable core model implies expansion velocities $\gtrsim$5 km s$^{-1}$. The first concern is this: if the internal velocity dispersion in Lupus is inherited from the turbulent motion inside the star-spawning core, how could the core remain intact for $\approx$10 Myr (see Ballesteros-Paredes [2006] for a theoretical study of this problem)? It is also remarkable that the WTTS population in Lupus is offset with respect to the dense molecular clouds and the nests of CTTS stars in the southwest direction and seems to be better aligned with the local part of the Gould Belt (Krautter et al. 1997). On the other extreme of the range of possible models, one could doubt that the older and the younger pre–main-sequence stars in Lupus were generated in the same kinematically coherent cloud or star-forming complex.

The main objective of this paper is to estimate the expansion rate (if any) of this very young association, making use of precision proper motions available in the Second US Naval Observatory CCD Astrograph Catalog (UCAC; Zacharias et al. 2004) and the convergent point method normally used for open clusters. That this is possible to do is an interesting find by itself, revealing the kinematical integrity of the association. In the absence of accurate trigonometric parallaxes, the convergent point method provides a good estimate of the depth of the association, i.e., the distribution of distances. Much improved distances to individual members allow me to revise the H-R diagram and consider the origin of the observed large spread of colors.

## 2. STARS

My selection of candidate members of the T association in Lupus is based on the list of 136 spectroscopically identified T Tauri stars in Krautter et al. (1997, their Table 5). The survey of Krautter et al. covers the area between $15^{\rm h}06^{\rm m}$ and $16^{\rm h}24^{\rm m}$ in right ascension and between $-47^\circ$ and $-32^\circ$ in declination. Their original selection is based on the *Röntgensatellit* (*ROSAT*) All-Sky Survey, as well as pointed observations in X-rays. They further select T Tauri–type stars from spectroscopic observations, requiring that the Li I $\lambda$6707 line be sufficiently strong ($W_{\rm Li6707} >$ 100 mÅ). CTTSs are differentiated from their WTTS counterparts by H$\alpha$ lines in emission. Note that Krautter et al. (1997) do not use any proper-motion or radial velocity data; therefore, the original sample in this paper is kinematically unbiased.

TABLE 1
STARS REJECTED AS KINEMATICAL NONMEMBERS OF THE LUPUS T ASSOCIATION

| Name | R.A. (ICRS) (deg) | Decl. (ICRS) (deg) | $(\mu_\alpha \cos\delta,\ \mu_\delta) \pm (\sigma_{\mu_{\alpha*}},\ \sigma_{\mu_\delta})$ (mas yr$^{-1}$) | $J$ (mag) | $H$ (mag) | $K_s$ (mag) |
|---|---|---|---|---|---|---|
| RX J1506.9−3714 | 226.7266292 | −37.2332795 | (−7.4, −1.4) ± (4.8, 4.8) | 11.192 | 10.538 | 10.407 |
| RX J1507.9−4515 | 226.9770712 | −45.2558956 | (25.6,−0.5) ± (1.7,1.4) | 9.417 | 8.995 | 8.919 |
| RX J1514.8−4220 | 228.7097224 | −42.3371912 | (−24.8, −4.0) ± (5.0, 5.0) | 12.214 | 11.835 | 11.749 |
| RX J1605.5−3846 | 241.3791324 | −38.7545706 | (5.1, 4.7) ± (5.0, 5.0) | 11.840 | 11.528 | 11.445 |
| RX J1506.9−3714 | 242.1345071 | −38.7870742 | (4.8, 2.4) ± (5.0, 5.0) | 12.974 | 12.183 | 12.076 |

The original 136 stars are cross-identified with the objects in the UCAC2 catalog (Zacharias et al. 2004) resulting in 98 objects. The rest of the T Tauri stars are not matched with any UCAC2 entries, because of their optical dimness. The positional mismatches between the *ROSAT* sources and their UCAC2 counterparts mostly fall well within 6″, with a few exceptions of up to 12″. The UCAC2 catalog provides astrometric proper motions for all cross-identified stars, along with estimated standard errors. It also includes $J$, $H$, and $K_s$ near-infrared magnitudes from the Two Micron All Sky Survey (2MASS). The majority of T Tauri stars identified in UCAC2 have similar proper motions, with an average of roughly $(\mu_{\alpha*},\ \mu_\delta) = (-17,\ -27)$ mas yr$^{-1}$. Assuming a systemic heliocentric tangential velocity of 22 km s$^{-1}$, the mean distance to the association is 145 pc, in close agreement with the estimations by Hughes et al. (1993) and Crawford (2000).

Five stars out of the 98 cross-identified objects in Lupus have proper motions from UCAC2, which are in obvious disagreement with the common streaming motion. They are listed in Table 1. The remaining 93 stars are considered bona fide kinematical members of the Lupus association. They are used in this paper for convergent point analysis and statistics estimation. Their names, International Celestial Reference System (ICRS) 2000 equatorial coordinates, proper motions with formal errors from UCAC2, photometric data from Wichmann et al. (1997) and 2MASS, and other parameters derived by me are specified in Table 2.

## 3. CONVERGENT POINT AND EXPANSION

In the idealized classical moving-cluster model, all member stars move with the same velocity with respect to a fixed, nonrotaing coordinate system. Their proper-motion vectors, extended along the great circles, intersect at a single point on the sky, called the convergent point. The direction to the convergent point is the true direction of the systemic velocity of the cluster. The importance of this direction arises from the simple equations that relate the angular distance ($\lambda$) between cluster members and the convergent point and the distance ($D$) to the observable radial velocity $V_r$, e.g.,

$$V_r = 4.74 \mu D \cot\lambda, \qquad (1)$$

where 4.74 is the astronomical unit in km s$^{-1}$ yr, $\mu$ is the magnitude of proper motion in mas yr$^{-1}$, $D$ is in kpc, and $V_r$ is in km s$^{-1}$. This equation can be written for each star, indicating a gradient in the radial velocities of individual members in the sky plane because of the finite extent of the cluster and the spread of $\lambda$. Alternatively, the heliocentric systemic velocity of the cluster, $V_c = V_r/\cos\lambda$, can be accurately determined if $\lambda$ is not too close to 90°. This derivation can be reversed, so that if the mean distance is known from other sources, the "true" astrometric radial velocity can be obtained, allowing us to study such astrophysical effects in radial velocities as the gravitational redshift and convection blueshift (Dravins et al. 1999). Finally, once the velocity of the cluster is determined, the spread of observed proper-motion magnitudes is directly related to the distribution of individual distances. Since the astrometric precision of proper motions is sufficiently high for nearby clusters, this method provides better defined H-R diagrams than assuming the same mean distance to all stars (e.g., de Bruijne 1999; de Bruijne et al. 2001). I use this option to estimate the depth of the Lupus association.

Things become complicated when a cluster (or an association) undergoes general expansion or contraction. Strictly linear radial motion from a common origin preserves the convergent point property, but the convergent point no longer corresponds to the systemic velocity direction (Blaauw 1964). Radial expansion moves the geometric convergent point farther from the cluster (to larger $\lambda$), while radial contraction moves it closer in (to smaller $\lambda$). This results in a detectable difference between the observed radial velocity and that derived from the geometric convergent point. Furthermore, in case of gravitationally unbound expanding associations, the effects of differential Galactic rotation and vertical acceleration should be taken into account (Makarov et al. 2004). The curvature of individual orbits becomes significant after several million years of expansion, and the convergent point loses focus and shifts.

The same technique of convergent point determination as that used for the Pleiades (Makarov & Robichon 2001) and $\alpha$ Persei (Makarov 2006) open clusters is applied here to the set of 93 Lupus stars in Table 2. This technique is based on the Amoeba algorithm of nonlinear optimization. The estimator function is the quadratic sum of weighted angular deviations of proper vector directions from the estimated direction to the convergent point, $\sum_i (\Delta_i/\sigma_{\Delta_i})^2$. Its global minimum provides an unbiased geometric estimate, independent of any astrophysical or dynamical assumptions about the stars. The estimated position of the convergent point and the 1 $\sigma$ error ellipse computed from the covariance matrix are depicted in the inset of Figure 1. The ICRS position of the convergent point is $(\alpha,\ \delta) = (92.8°,\ -28.1°) \pm (3.1°,\ 5.0°)$. The error ellipse is strongly elongated along the great circle connecting the geometric center of the association with the convergent point, because of the shallow angles at which the individual great circles of proper motions intersect. Therefore, the largest error arises from the estimation of the angular distance between the center and the convergent point, i.e., $\lambda = 104.7° \pm 5.7°$.

Assuming a mean heliocentric velocity of 22 km s$^{-1}$, the estimated $\lambda$ leads to a negative mean radial velocity of −5.6 km s$^{-1}$. The observed systemic radial velocity is $+2.6 \pm 1.8$ km s$^{-1}$ (James et al. 2006). In other terms, the measured $\lambda$ (from the geometric convergent point) is larger than the inferred value (from the radial velocity) by $21.5° \pm 7.4°$. This difference implies a weak degree of expansion. For comparison, if the Lupus association had the same rate of expansion as found for the dispersed TW Hya association in the vicinity of the Sun with initial relative

TABLE 2

KINEMATIC T TAURI MEMBERS OF THE LUPUS ASSOCIATION

| Name (1) | R.A. (ICRS) (deg) (2) | Decl. (ICRS) (deg) (3) | $(\mu_\alpha \cos\delta,\ \mu_\delta) \pm (\sigma_{\mu_{\alpha*}},\ \sigma_{\mu_\delta})$ (mas yr$^{-1}$) (4) | $D_{\rm kin}$ (pc) (5) | $\Delta/\sigma_\Delta$ (6) | $v_\perp$ (km s$^{-1}$) (7) | $V$ (mag) (8) | $B-V$ (mag) (9) | $U-B$ (mag) (10) | $V-R_{\rm c}$ (mag) (11) | $V-I_{\rm c}$ (mag) (12) | $J$ (mag) (13) | $H$ (mag) (14) | $K_s$ (mag) (15) |
|---|---|---|---|---|---|---|---|---|---|---|---|---|---|---|
| RX J1505.9−4311 | 226.4868880 | −43.2008706 | (−25.5, −26.0) ± (2.9, 2.6) | 126 | 1.0 | 1.7 | 12.58 | 1.35 | 1.25 | 0.83 | 1.63 | 9.893 | 9.209 | 9.039 |
| RX J1507.2−3505 | 226.8117345 | −35.0832037 | (−33.1, −29.4) ± (1.5, 1.8) | 102 | 3.6 | 3.0 | 10.53 | 0.88 | 0.43 | 0.51 | 0.96 | 8.893 | 8.416 | 8.336 |
| RX J1507.4−4601 | 226.8649380 | −46.0187089 | (−18.5, −17.7) ± (2.5, 3.6) | 180 | 1.0 | 2.6 | ... | ... | ... | ... | ... | 9.735 | 9.284 | 9.131 |
| RX J1507.6−4603 | 226.9072486 | −46.0543398 | (−20.3, −22.7) ± (1.5, 2.9) | 152 | 0.6 | 0.9 | 11.64 | 0.97 | 0.60 | 0.57 | 1.12 | 9.821 | 9.211 | 9.098 |
| RX J1508.6−4423 | 227.1572383 | −44.3880678 | (−19.7, −20.8) ± (1.5, 3.5) | 161 | 0.8 | 1.6 | 10.63 | 0.69 | 0.14 | 0.41 | 0.80 | 9.359 | 8.925 | 8.809 |
| HD 133938 | 227.1604362 | −44.0144759 | (−22.7, −24.7) ± (1.8, 2.3) | 137 | 0.9 | 1.2 | 10.39 | 0.71 | 0.16 | 0.42 | 0.83 | 8.950 | 8.518 | 8.446 |
| RX J1508.8−3715 | 227.2241500 | −37.2630187 | (−17.6, −27.8) ± (3.2, 2.0) | 138 | −1.5 | −2.9 | ... | ... | ... | ... | ... | 9.767 | 9.146 | 9.002 |
| RX J1511.0−3251 | 227.7687512 | −32.8584587 | (−23.6, −26.0) ± (2.8, 2.8) | 128 | 0.5 | 0.8 | 11.92 | 1.23 | 1.01 | 0.76 | 1.48 | 9.467 | 8.770 | 8.670 |
| RX J1511.6−3550 | 227.9040253 | −35.8449345 | (−20.1, −24.4) ± (4.7, 4.7) | 143 | −0.0 | −0.1 | 12.59 | 1.10 | 0.91 | 0.68 | 1.38 | 10.101 | 9.523 | 9.331 |
| HD 134974 | 228.5314383 | −41.0600470 | (−17.4, −27.4) ± (1.7, 1.8) | 141 | −2.0 | −2.3 | 10.38 | 0.61 | 0.04 | 0.36 | 0.74 | 9.142 | 8.721 | 8.570 |
| HD 135127 | 228.6649286 | −34.7614823 | (−17.5, −23.8) ± (1.3, 1.1) | 152 | −1.2 | −1.1 | 9.63 | 0.30 | −0.06 | 0.30 | 0.61 | 8.235 | 8.036 | 7.988 |
| RX J1515.7−3331 | 228.9390568 | −33.5332609 | (−21.5, −29.3) ± (2.8, 1.7) | 123 | −0.8 | −1.1 | 10.69 | 0.88 | 0.43 | 0.52 | 1.00 | 8.981 | 8.461 | 8.384 |
| RX J1515.8−4418 | 228.9697465 | −44.3048142 | (−18.9, −21.5) ± (2.6, 2.4) | 161 | 0.7 | 1.3 | 12.68 | 1.11 | 0.85 | 0.65 | 1.35 | 10.181 | 9.573 | 9.454 |
| RX J1516.6−4406 | 229.1526542 | −44.1223562 | (−17.9, −21.9) ± (1.8, 1.5) | 163 | 0.4 | 0.5 | 11.93 | 1.04 | 0.75 | 0.64 | 1.20 | 9.898 | 9.316 | 9.193 |
| RX J1518.4−3738 | 229.6121453 | −37.6339217 | (−20.6, −28.2) ± (1.6, 1.6) | 130 | −0.8 | −0.7 | 10.92 | 0.87 | 0.44 | 0.51 | 1.01 | 9.081 | 8.618 | 8.506 |
| RX J1518.8−4050 | 229.7200809 | −40.8480006 | (−14.4, −20.0) ± (2.5, 2.4) | 185 | −0.3 | −0.7 | 11.01 | 0.91 | 0.48 | 0.53 | 1.04 | 9.145 | 8.659 | 8.547 |
| RX J1519.2−4056 | 229.8166730 | −40.9354437 | (−24.6, −30.2) ± (3.3, 1.4) | 117 | 0.4 | 0.6 | ... | ... | ... | ... | ... | 9.549 | 9.021 | 8.830 |
| RX J1522.2−3959 | 230.5483980 | −39.9974964 | (−23.6, −23.5) ± (3.3, 2.5) | 137 | 1.6 | 3.0 | 12.02 | 1.07 | 0.77 | 0.65 | 1.29 | 9.906 | 9.297 | 9.100 |
| RX J1523.4−4055 | 230.8565698 | −40.9296662 | (−26.5, −27.3) ± (2.5, 2.4) | 120 | 2.0 | 2.8 | 11.87 | 1.03 | 0.70 | 0.63 | 1.16 | 9.957 | 9.389 | 9.260 |
| RX J1524.0−3209 | 231.0127042 | −32.1641339 | (−20.6, −28.1) ± (2.8, 2.8) | 127 | −0.4 | −0.6 | 12.38 | 1.25 | 1.06 | 0.82 | 1.73 | 9.502 | 8.817 | 8.644 |
| RX J1524.5−3652 | 231.1348262 | −36.8674398 | (−20.1, −24.4) ± (1.6, 1.7) | 143 | 0.8 | 0.9 | 11.30 | 0.91 | 0.48 | 0.52 | 1.01 | 9.549 | 9.049 | 8.930 |
| RX J1525.0−3604 | 231.2648874 | −36.0793006 | (−19.6, −29.4) ± (1.6, 1.6) | 127 | −1.3 | −1.3 | 10.92 | 0.96 | 0.55 | 0.57 | 1.09 | 8.998 | 8.465 | 8.320 |
| HD 137059 | 231.3208380 | −38.7572489 | (−31.3, −40.0) ± (1.6, 2.4) | 89 | 0.6 | 0.5 | 8.75 | 0.67 | 0.14 | 0.40 | 0.76 | 7.410 | 7.100 | 6.986 |
| RX J1525.5−3613 | 231.3881674 | −36.2296789 | (−17.4, −23.5) ± (3.0, 3.0) | 154 | −0.1 | −0.2 | 11.59 | 0.98 | 0.60 | 0.62 | 1.21 | 9.564 | 9.004 | 8.842 |
| RX J1525.6−3537 | 231.4027836 | −35.6255289 | (−21.7, −24.1) ± (4.8, 4.8) | 138 | 0.6 | 1.8 | 12.44 | 1.24 | 0.93 | 0.80 | 1.59 | 9.780 | 9.135 | 8.963 |
| RX J1526.0−4501 | 231.4985203 | −45.0210623 | (−22.6, −21.8) ± (1.4, 1.5) | 146 | 3.8 | 3.8 | 10.87 | 0.79 | 0.31 | 0.45 | 0.87 | 9.443 | 8.984 | 8.901 |
| RX J1526.8−3721 | 231.7190750 | −37.3683939 | (−26.5, −37.6) ± (4.9, 4.9) | 98 | −0.2 | −0.5 | 13.02 | 1.40 | 1.05 | 0.89 | 1.85 | 9.981 | 9.319 | 9.141 |
| RX J1529.3−3737 | 232.3291415 | −37.6223437 | (−28.7, −32.6) ± (4.9, 4.9) | 104 | 0.8 | 2.0 | 13.72 | 1.52 | 1.04 | 0.99 | 2.36 | 9.928 | 9.282 | 9.012 |
| RX J1529.6−3546 | 232.4107539 | −35.7809520 | (−20.9, −28.0) ± (1.6, 1.6) | 128 | 0.2 | 0.2 | ... | ... | ... | ... | ... | 8.788 | 8.257 | 8.119 |
| RX J1529.7−3628 | 232.4469374 | −36.4770578 | (−20.3, −21.6) ± (2.8, 2.8) | 151 | 1.3 | 2.6 | ... | ... | ... | ... | ... | 9.643 | 9.106 | 8.970 |
| RX J1529.8−4522 | 232.4536589 | −45.3793889 | (−13.1, −24.5) ± (1.9, 1.5) | 165 | −1.9 | −2.7 | ... | ... | ... | ... | ... | 10.041 | 9.384 | 9.251 |
| RX J1531.3−3329 | 232.8413674 | −33.4942903 | (−25.2, −31.3) ± (1.5, 1.5) | 110 | 1.2 | 0.9 | ... | ... | ... | ... | ... | 9.391 | 8.941 | 8.801 |
| RX J1533.0−3930 | 233.2384433 | −39.5122281 | (−12.1, −37.4) ± (5.0, 5.0) | 115 | −2.4 | −6.5 | 13.10 | 1.51 | 1.32 | 0.96 | 1.98 | 9.851 | 9.144 | 8.946 |
| RX J1534.1−3916 | 233.5306695 | −39.2714545 | (−24.1, −26.2) ± (1.8, 1.9) | 127 | 2.6 | 2.9 | 10.79 | 0.84 | 0.38 | 0.49 | 0.95 | 9.141 | 8.646 | 8.553 |
| RX J1534.3−3300 | 233.6590077 | −40.0411334 | (−26.3, −34.1) ± (2.8, 2.7) | 105 | 0.8 | 1.1 | ... | ... | ... | ... | ... | 9.554 | 8.908 | 8.754 |
| RX J1534.6−4002 | 233.8493524 | −44.2095950 | (−21.7, −18.7) ± (5.3, 5.0) | 160 | 1.5 | 5.7 | 11.98 | 1.23 | 1.03 | 0.76 | 1.45 | 11.631 | 10.958 | 10.725 |
| RX J1535.4−4412 | 234.5110506 | −38.1230709 | (−17.6, −21.8) ± (3.7, 3.4) | 161 | 0.6 | 1.7 | ... | ... | ... | ... | ... | 10.112 | 9.572 | 9.376 |
| RX J1538.0−3807 | 234.6594718 | −39.2820423 | (−20.2, −31.5) ± (1.6, 2.2) | 121 | −0.5 | −0.5 | ... | ... | ... | ... | ... | 9.594 | 9.008 | 8.854 |
| RX J1538.6−3916 | 234.6794474 | −44.1965114 | (−21.7, −29.3) ± (1.5, 1.2) | 125 | 1.3 | 1.1 | ... | ... | ... | ... | ... | 8.805 | 8.344 | 8.210 |
| RX J1538.7−4411 | 234.9432227 | −34.8507028 | (−20.1, −19.7) ± (2.7, 2.7) | 158 | 2.0 | 4.1 | 10.56 | 0.85 | 0.36 | 0.49 | 0.98 | 9.631 | 8.993 | 8.861 |
| RX J1539.7−3450 | 235.0101724 | −46.5718650 | (−23.0, −18.8) ± (3.1, 2.8) | 155 | 3.1 | 6.7 | ... | ... | ... | ... | ... | 9.861 | 9.284 | 9.117 |
| RX J1540.0−4634 | 235.1715433 | −37.9384845 | (−21.7, −31.3) ± (5.0, 5.0) | 118 | 0.1 | 0.3 | ... | ... | ... | ... | ... | 9.927 | 9.324 | 9.187 |
| RX J1540.7−3756 | 235.5216086 | −36.0255025 | (−27.6, −32.3) ± (4.8, 4.8) | 105 | 1.0 | 2.5 | 12.35 | 1.19 | 1.05 | 0.74 | 1.42 | 9.919 | 9.250 | 9.088 |
| RX J1542.0−3601 | 236.0156900 | −33.1864356 | (−22.5, −28.2) ± (1.5, 1.5) | 122 | 1.9 | 1.7 | ... | ... | ... | ... | ... | 9.062 | 8.546 | 8.414 |
| RX J1544.0−3311 | 236.1963315 | −38.1945989 | (−24.0, −21.5) ± (2.9, 2.8) | 139 | 3.0 | 5.6 | ... | ... | ... | ... | ... | 9.249 | 8.590 | 8.505 |
| RX J1544.8−3811 | 236.4676824 | −42.3712237 | (−17.7, −29.2) ± (1.2, 1.1) | 133 | −0.6 | −0.4 | ... | ... | ... | ... | ... | 8.673 | 8.081 | 7.933 |

TABLE 2—*Continued*

| Name (1) | R.A. (ICRS) (deg) (2) | Decl. (ICRS) (deg) (3) | $(\mu_\alpha \cos\delta,\ \mu_\delta) \pm (\sigma_{\mu_{\alpha*}},\ \sigma_{\mu_\delta})$ (mas yr$^{-1}$) (4) | $D_{\rm kin}$ (pc) (5) | $\Delta/\sigma_\Delta$ (6) | $v_\perp$ (km s$^{-1}$) (7) | $V$ (mag) (8) | $B-V$ (mag) (9) | $U-B$ (mag) (10) | $V-R_{\rm c}$ (mag) (11) | $V-I_{\rm c}$ (mag) (12) | $J$ (mag) (13) | $H$ (mag) (14) | $K_s$ (mag) (15) |
|---|---|---|---|---|---|---|---|---|---|---|---|---|---|---|
| RX J1545.9−4222 | 236.6716715 | −36.3131756 | (−16.1, −25.9) ± (3.3, 1.6) | 146 | −0.2 | −0.4 | 10.59 | 0.99 | 0.63 | 0.59 | 1.15 | 9.490 | 8.947 | 8.783 |
| RX J1546.6−3618 | 236.9240148 | −40.3074395 | (−18.5, −26.2) ± (1.4, 1.8) | 141 | 1.1 | 1.1 | 11.28 | 0.89 | 0.41 | 0.53 | 1.07 | 9.294 | 8.811 | 8.662 |
| RX J1547.6−4018[a] | 237.0088868 | −40.0743464 | (−14.7, −13.6) ± (5.0, 5.0) | 225 | 1.1 | 5.6 | 11.08 | 0.95 | 0.61 | 0.55 | 1.05 | 9.621 | 8.995 | 8.777 |
| RX J1548.0−4004 | 237.1751748 | −43.5891212 | (−12.5, −18.5) ± (3.8, 1.4) | 204 | 0.3 | 0.9 | 12.50 | 1.30 | 1.08 | 0.82 | 1.75 | 9.951 | 9.475 | 9.324 |
| RX J1548.6−4335[a] | 237.1771909 | −35.3352031 | (−15.4, −24.2) ± (4.8, 4.9) | 154 | −0.0 | −0.1 | ... | ... | ... | ... | ... | 10.147 | 9.360 | 9.041 |
| RX J1548.7−3520 | 237.4374100 | −39.4192003 | (−19.7, −25.9) ± (1.3, 1.3) | 138 | 2.3 | 2.0 | ... | ... | ... | ... | ... | 8.833 | 8.266 | 8.141 |
| HD 141277 | 237.4967074 | −36.4992825 | (−18.7, −22.2) ± (3.2, 2.4) | 153 | 1.4 | 2.9 | 10.55 | 0.92 | 0.51 | 0.53 | 1.03 | 9.560 | 9.021 | 8.884 |
| RX J1549.9−3629[a] | 237.6946756 | −38.4907842 | (−8.9, −16.9) ± (5.0, 5.0) | 235 | −0.3 | −1.5 | 11.52 | 0.98 | 0.63 | 0.57 | 1.11 | 9.876 | 9.115 | 8.899 |
| RX J1552.3−3819 | 238.0813427 | −38.3253784 | (−17.4, −25.0) ± (5.0, 5.0) | 147 | 0.4 | 1.2 | 13.19 | 1.27 | 1.34 | 0.76 | 1.64 | 10.359 | 9.681 | 9.525 |
| RX J1554.4−3759 | 238.6124403 | −37.9963470 | (−12.9, −21.2) ± (4.9, 4.9) | 180 | 0.0 | 0.1 | ... | ... | ... | ... | ... | 10.918 | 10.313 | 10.054 |
| RX J1555.4−3338 | 238.8592489 | −33.6398037 | (−16.2, −33.9) ± (3.6, 3.5) | 116 | −1.1 | −2.2 | 12.45 | 1.13 | 0.93 | 0.71 | 1.40 | 10.158 | 9.540 | 9.353 |
| RX J1555.5−3709 | 238.8908145 | −37.1614103 | (−17.0, −28.5) ± (4.7, 4.7) | 134 | −0.0 | −0.1 | 12.52 | 1.23 | 1.02 | 0.75 | 1.48 | 9.964 | 9.327 | 9.165 |
| RX J1556.0−3655[a] | 239.0087471 | −36.9245214 | (−9.1, −25.6) ± (4.6, 4.6) | 163 | −1.2 | −4.2 | 13.85 | 1.20 | −0.14 | 0.94 | 1.99 | 10.396 | 9.595 | 9.303 |
| CD −36 10569 | 239.9562953 | −36.4744234 | (−27.7, −45.5) ± (1.9, 1.3) | 83 | 0.6 | 0.4 | 11.00 | 1.12 | 0.89 | 0.68 | 1.34 | 8.773 | 8.150 | 8.029 |
| RX J1559.9−3750[a] | 239.9757183 | −37.8463559 | (−12.3, −22.3) ± (5.0, 5.0) | 175 | −0.1 | −0.4 | 13.03 | 1.57 | 1.24 | 0.80 | 2.06 | 9.616 | 8.878 | 8.659 |
| RX J1601.1−3320 | 240.2873721 | −33.3372864 | (−12.2, −22.8) ± (1.7, 1.5) | 168 | −0.7 | −0.9 | 10.88 | 0.89 | 0.34 | 0.53 | 1.07 | 9.027 | 8.552 | 8.528 |
| RX J1601.8−4026 | 240.4559330 | −40.4386925 | (−14.6, −19.5) ± (2.9, 2.6) | 184 | 1.1 | 2.8 | ... | ... | ... | ... | ... | 9.842 | 9.230 | 9.057 |
| RX J1601.9−3613 | 240.4965965 | −36.2154462 | (−15.2, −33.0) ± (2.1, 1.7) | 121 | −1.6 | −1.9 | 11.96 | 1.06 | 0.73 | 0.67 | 1.39 | 9.599 | 8.972 | 8.854 |
| RX J1603.2−3239 | 240.7992148 | −32.6556403 | (−12.4, −29.9) ± (4.9, 4.9) | 133 | −0.9 | −2.8 | 12.94 | 1.31 | 0.88 | 0.80 | 1.69 | 9.979 | 9.293 | 9.124 |
| HD 143677[a] | 240.9390300 | −43.9303428 | (−12.9, −23.7) ± (1.0, 1.3) | 168 | 0.0 | 0.0 | 9.67 | 0.92 | 0.50 | 0.53 | 1.02 | 7.927 | 7.413 | 7.314 |
| RX J1603.8−3938 | 240.9687409 | −39.6503531 | (−17.6, −28.7) ± (3.2, 1.4) | 133 | 0.5 | 0.9 | 11.02 | 1.05 | 0.76 | 0.64 | 1.23 | 8.941 | 8.355 | 8.224 |
| RX J1604.5−3207 | 241.1273359 | −32.1246328 | (−14.2, −23.2) ± (3.9, 3.2) | 158 | 0.2 | 0.5 | 10.86 | 0.89 | 0.44 | 0.50 | 1.02 | 9.168 | 8.690 | 8.565 |
| HD 143978 | 241.2378056 | −38.9543623 | (−27.2, −47.6) ± (1.0, 1.1) | 81 | 0.8 | 0.3 | 9.36 | 0.47 | −0.08 | 0.39 | 0.74 | 8.143 | 7.973 | 7.857 |
| RX J1605.5−3837 | 241.3887195 | −38.6292164 | (−7.9, −17.4) ± (5.0, 5.0) | 233 | −0.3 | −1.6 | ... | ... | ... | ... | ... | 10.785 | 10.100 | 9.903 |
| RX J1605.7−3905 | 241.4375150 | −39.1018212 | (−15.9, −30.3) ± (1.4, 1.5) | 130 | −0.4 | −0.4 | 10.49 | 0.80 | 0.31 | 0.47 | 0.90 | 8.910 | 8.523 | 8.362 |
| RX J1606.3−4447 | 241.5972877 | −44.7932092 | (−17.5, −26.5) ± (3.0, 2.7) | 143 | 1.0 | 2.1 | ... | ... | ... | ... | ... | 10.230 | 9.571 | 9.426 |
| RX J1607.2−3839[a] | 241.8070750 | −38.6566334 | (−9.0, −17.6) ± (5.0, 5.0) | 225 | −0.1 | −0.5 | 12.76 | 1.35 | 1.11 | 0.89 | 1.81 | 9.691 | 8.960 | 8.875 |
| RX J1608.0−3857[a] | 241.9998836 | −38.9641687 | (−12.8, −23.3) ± (5.0, 5.0) | 167 | 0.0 | 0.2 | 12.77 | 1.43 | 0.96 | 0.91 | 1.91 | 9.642 | 8.953 | 8.703 |
| F 304 | 242.0456774 | −39.1794367 | (−10.9, −24.2) ± (5.0, 5.0) | 168 | −0.4 | −1.5 | 12.84 | 1.24 | 1.07 | 0.78 | 1.46 | 10.389 | 9.764 | 9.609 |
| RX J1608.3−3843 | 242.0759833 | −38.7348031 | (−14.7, −31.0) ± (3.7, 3.4) | 129 | −0.5 | −1.1 | 12.23 | 1.28 | 1.03 | 0.80 | 1.63 | 9.564 | 8.919 | 8.714 |
| RX J1608.5−3847[a] | 242.1315033 | −38.7914620 | (−9.6, −23.6) ± (5.0, 5.0) | 175 | −0.5 | −2.2 | ... | ... | ... | ... | ... | 9.676 | 8.926 | 8.623 |
| RX J1608.6−3922[a] | 242.1507618 | −39.3840295 | (−6.3, −24.5) ± (5.0, 5.0) | 176 | −1.2 | −5.0 | 13.48 | 1.52 | 1.01 | 1.01 | 2.03 | 9.884 | 9.043 | 8.658 |
| RX J1608.9−3945 | 242.2262039 | −39.7679834 | (−5.8, −29.3) ± (5.1, 5.0) | 149 | −1.7 | −6.2 | 15.33 | 3.35 | ... | 1.07 | 2.76 | 10.851 | 10.141 | 9.934 |
| RX J1608.9−3905 | 242.2261359 | −39.1016273 | (−10.9, −27.6) ± (2.3, 2.3) | 150 | −1.5 | −2.4 | 10.88 | 1.03 | 0.66 | 0.60 | 1.14 | 8.909 | 8.375 | 8.212 |
| RX J1609.4−3850[a] | 242.3641533 | −38.8386145 | (−3.7, −23.6) ± (5.0, 5.0) | 186 | −1.6 | −7.0 | 12.72 | 1.39 | 1.17 | 0.91 | 1.97 | 9.462 | 8.831 | 8.567 |
| RX J1610.0−4016 | 242.5199421 | −40.2700839 | (−16.4, −28.5) ± (1.4, 3.7) | 136 | 0.6 | 0.8 | 11.20 | 0.97 | 0.59 | 0.56 | 1.09 | 9.339 | 8.796 | 8.619 |
| RX J1611.6−3841 | 242.9084274 | −38.6932412 | (−13.3, −23.1) ± (5.0, 5.0) | 166 | 0.2 | 0.9 | 13.40 | 1.91 | 1.74 | 1.12 | 2.18 | 10.912 | 10.233 | 10.055 |
| RX J1612.0−3840[a] | 243.0058756 | −38.6743331 | (−5.6, −25.5) ± (2.7, 3.0) | 170 | −2.5 | −5.5 | 11.69 | 1.30 | 1.13 | 0.82 | 1.60 | 9.057 | 8.432 | 8.179 |
| RX J1613.0−4004[a] | 243.2600659 | −40.0758150 | (−13.5, −34.4) ± (5.0, 5.0) | 121 | −0.7 | −2.1 | 13.49 | 1.61 | 1.38 | 0.98 | 2.1 | 9.866 | 9.071 | 8.828 |
| RX J1613.1−3804 | 243.3028571 | −38.0642498 | (−17.0, −25.4) ± (3.2, 1.6) | 145 | 1.2 | 2.4 | ... | ... | ... | ... | ... | 9.677 | 9.029 | 8.880 |
| RX J1614.4−3808 | 243.6098856 | −38.1332339 | (−16.0, −23.0) ± (5.0, 5.0) | 158 | 0.8 | 2.9 | ... | ... | ... | ... | ... | 9.953 | 9.308 | 9.121 |
| RX J1615.3−3255[a] | 243.8342971 | −32.9180823 | (−10.3, −21.0) ± (4.5, 4.5) | 184 | −0.1 | −0.6 | 12.00 | 1.22 | 0.66 | 0.79 | 1.50 | 9.435 | 8.777 | 8.558 |
| RX J1615.9−3241 | 243.9873453 | −32.6903070 | (−24.9, −40.6) ± (2.8, 2.8) | 90 | 1.2 | 1.4 | ... | ... | ... | ... | ... | 9.978 | 9.361 | 9.207 |
| HD 147048 | 245.3008215 | −40.5057225 | (−7.9, −28.5) ± (1.0, 1.0) | 151 | −5.1 | −3.6 | 10.45 | 0.82 | 0.37 | 0.49 | 0.89 | 8.964 | 8.568 | 8.465 |
| HD 147402 | 245.8731424 | −39.9668914 | (−12.2, −27.2) ± (1.3, 2.2) | 149 | −0.3 | −0.3 | 10.82 | 0.67 | 0.14 | 0.42 | 0.79 | 9.466 | 9.094 | 8.983 |
| SAO 207620 | 245.9068348 | −34.6727323 | (−13.6, −32.6) ± (1.2, 1.3) | 122 | −1.5 | −1.1 | ... | ... | ... | ... | ... | 8.278 | 7.934 | 7.842 |
| HD 147454 | 245.8846189 | −34.6638795 | (−15.5, −28.9) ± (1.0, 1.1) | 131 | 1.4 | 0.9 | ... | ... | ... | ... | ... | 8.312 | 8.071 | 8.016 |

[a] Stars whose location on the near-infrared H-R diagram suggests they may be as young as 1 Myr.

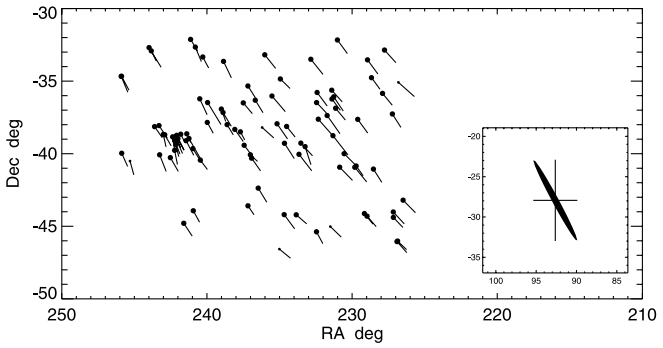


FIG. 1.—ICRS positions and proper motions of pre–main-sequence stars in the Lupus T association. Kinematically outlying stars are indicated by smaller dots. The typical length of proper-motion vectors is 31 mas yr$^{-1}$. *Inset*: Convergent point of the association (in the crosshairs), the 1 $\sigma$ error ellipse, and the projected coordinate error bars, as geometrically determined by the Amoeba algorithm.

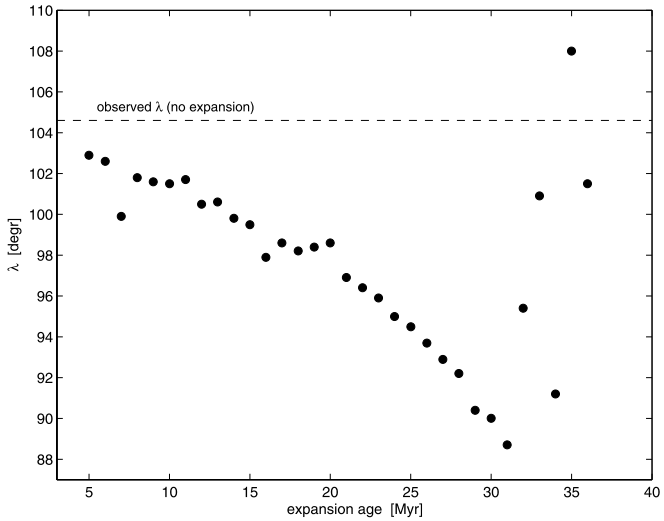


FIG. 2.—Angular separations $\lambda$ between the direction to the center of the Lupus association and the direction of its motion, computed for a grid of expansion ages. The geometrically determined value of $\lambda$ based on observed proper motions not corrected for expansion is shown with the dashed line.

velocities of stars at $\simeq$7 km s$^{-1}$ (Makarov et al. 2005), the geometric convergent point would be farther out by roughly 50°. I seek to learn whether the slow rate of expansion in the observed proper-motion field of Lupus is consistent with the size of this association and its estimated age.

If it is assumed that the association emerged from a compact star-forming region and expanded into the present volume, the model of freely expanding gravitationally unbound groups, developed in (Makarov et al. 2004), is applicable. In particular, their equations (9) and (13) specify distance-independent corrections to observed proper motions that should be applied in order to restore the "true" direction of the systemic motion through the convergent point, eliminating the effects of expansion, differential Galactic rotation, and vertical oscillation to a first-order approximation. These corrections are functions of galactic coordinates and the expansion age, which enters as a free parameter. Since the age of Lupus stars is not accurately known, I compute the proper-motion corrections for a grid of ages 5, 6, . . . , 36 Myr, run the convergent point estimation program, and derive the angle $\lambda$ between the cluster and the convergent point. The result is depicted in Figure 2. It shows that the required $\lambda_{\rm RV} = 83.2^\circ$ is never actually achieved, but the closest it comes is at $T_{\rm expasn} \simeq$ 30 Myr. Given the astrometric data, it would have taken the Lupus association 30 Myr to expand to a fraction of its current extent on the sky, if it diverged from a common compact core. There is little doubt that the Lupus stars are much younger, since the isochrone estimates from Wichmann et al. (1997) range between 0.6 and 6 Myr for the CTTSs and between 1 and 16 Myr for the WTTSs, with an overall median of roughly 6 Myr. The shift of the convergent point implies that the velocity of expansion in Lupus is $\lesssim$1 km s$^{-1}$. The apparent extent of the association is approximately 15°, or 40 pc, at a distance of 145 pc. Hence, the association could grow in size by roughly 12 pc in 6 Myr, and the initial size of the star-forming region was at least 28 pc. This estimate is probably understated, because the distribution of members in the sky (Fig. 1) suggests that the association extends beyond the boundaries of the spectroscopically surveyed area, and we find a depth of the association much larger than 40 pc in § 4. The conclusion is that the Lupus stars emerged from multiple star-forming cores spread over $\approx$30 pc or more in space.

## 4. DISTRIBUTIONS OF INTERNAL VELOCITIES, DISTANCES, AND AGES

Internal velocity dispersions (standard deviation in one coordinate component) are determined to be well below 1 km s$^{-1}$ in the Hyades and the Pleiades. In dynamically relaxed open clusters, this parameter is related to the total mass, predicated on dynamical models. Associations of stars are not gravitationally bound, and, of course, not dynamically relaxed. The velocity dispersion of an association is determined by the relative motion of the protostellar cores inside the star-forming cloud and by the breakup of nonhierarchical multiple systems. The total velocity dispersion as observed is the quadratic sum of this physical intrinsic dispersion and the stochastic dispersion coming from the astrometric measurement error. We are interested in the former and, therefore, have to estimate the contribution of the latter. Once the convergent point is known, the total velocity dispersion is derived from the distribution of the transverse tangential velocity components $v_\perp$ (Makarov & Robichon 2001), which are orthogonal to the great circles connecting the stars and the convergent point and lie in the plane of the sky. These transverse components, in km s$^{-1}$, are computed from the deviations of proper-motion vectors $\Delta$ using the moving-cluster distances, which are, in their turn, based on the proper-motion components along the connecting great circles. In this way, observed proper-motion vectors are completely utilized to produce essential physical parameters.

Unless the intrinsic velocity dispersion is as large as several km s$^{-1}$, this determination is limited by the available astrometric precision. Figure 3*a* depicts the distribution of residual relative angular deviations $\Delta_i/\sigma_{\Delta_i}$ for the Lupus stars, specified in Table 2. The meaning of this distribution is rather technical, but it is needed to estimate the contribution of expected proper-motion errors. The histogram is fitted by a Gaussian of standard deviation 1.04. It is noted that the astrometric measurement error is assumed to have a Gaussian distribution, which justifies this fit. The distribution of intrinsic velocities, on the contrary, is likely to be non-Gaussian, but rather composed of different substructures for nonrelaxed systems. In fact, given sufficiently accurate proper motions, individual members could be traced to their native cores. We are not yet at this level of astrometric precision, and the standard deviation of 1.04 on $\Delta_i/\sigma_{\Delta_i}$ indicates that the measurement error is the dominant constituent of the observed dispersion (the $\sigma$ equals exactly 1 if the intrinsic dispersion is zero). Therefore, most of the scatter in the measured transverse velocities $v_\perp$ is expected to come from the measurement errors. Keeping that in mind, we proceed to the histogram of transverse velocities in Figure 3*b*. The Gaussian fit yields a surprisingly small standard deviation of

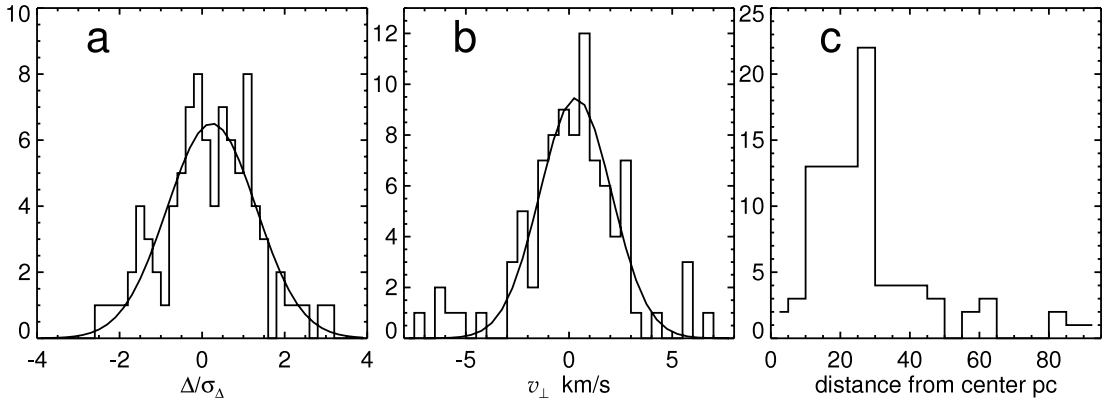


FIG. 3.—Distributions of (*a*) relative angular deviations of proper-motion vectors from the common convergent point, (*b*) absolute transverse tangential velocities in km $s^{-1}$, and (*c*) distances relative to the association's center in parsecs. Gaussian fits are shown for the former two histograms.

1.3 km $s^{-1}$. Taking into account the contribution of astrometric errors, the physical dispersion per coordinate must be significantly smaller than 1 km $s^{-1}$. However, we may be seeing the contribution of possibly non-Gaussian intrinsic velocities in this distribution. A robust estimate of the total observed dispersion as the half-difference of the 0.84 and 0.16 quantiles yields a substantially larger 2.1 km $s^{-1}$. In the event that the proper-motion errors are strongly overestimated in the catalog, the upper limit on the intrinsic dispersion is set at $\approx$1.3 km $s^{-1}$. This makes the Lupus T association similar to the $\alpha$ Per cluster, where a velocity dispersion below the detection limit was found (Makarov 2006).

Let us consider now the distribution of ages. The isochrone estimates by Wichmann et al. (1997) demonstrate a large spread, with nearly half of the CTTSs being younger than 1 Myr and several WTTSs being as old as 25–30 Myr. Their work also indicates that the more massive stars are on average older than the less massive stars. Their analysis is hampered by the large spread of individual distances. Using the moving-cluster method in its classical form (§ 3), I estimate the distances to all members listed in Table 2. The histogram of distances is presented in Figure 3*c*. Typical errors range from 7 to 40 pc, as defined by the proper-motion errors (between 1 and 5 mas $yr^{-1}$). The distribution indicates a total depth of at least 80 pc, assuming that the tails are made of astrometric outliers. Half of the identified members are located in a sphere of radius 26 pc, and 75% are in a sphere of radius 32 pc. Thus, many more T Tauri stars are expected to lie outside the boundaries of the available survey.

The distances deduced from the moving-cluster method, imprecise as they are for some of the stars, should be taken into account in constructing a H-R diagram and estimating ages. When I embarked on this task, I expected to see a smaller spread across the isochrones, indicating more clearly the age of the association. The outcome baffled these expectations. Figure 4 displays the H-R diagram of the 93 Lupus members in the near-infrared magnitudes $J$ and $K_s$ from 2MASS when the same distance of 145 pc is assumed for all stars (Fig. 4, *left*) and when individual distances specified in Table 2 are utilized (Fig. 4, *right*). The spurious "horizontal sequence" around $M_{K_s} \approx 3$ in the left plot is gone, but a considerable scatter along the $(J - K_s)$ axis remains. Differential extinction may contribute to this scatter, because some of the stars may be behind the Lupus clouds. According to Wichmann et al. (1997), the extinction $A_V$ for our stars rarely exceeds 0.9 mag; thus, the extinction $A_{K_s}$ should be generally less than 0.1 mag. It appears that most of the spread in the diagram corresponds to the actual distribution of ages. The most prominent feature of the diagram based on the corrected distances is the group of very red stars around the 1 Myr isochrone from Siess et al. (2000) separated by a clear swath from the rest of the association. These stars are

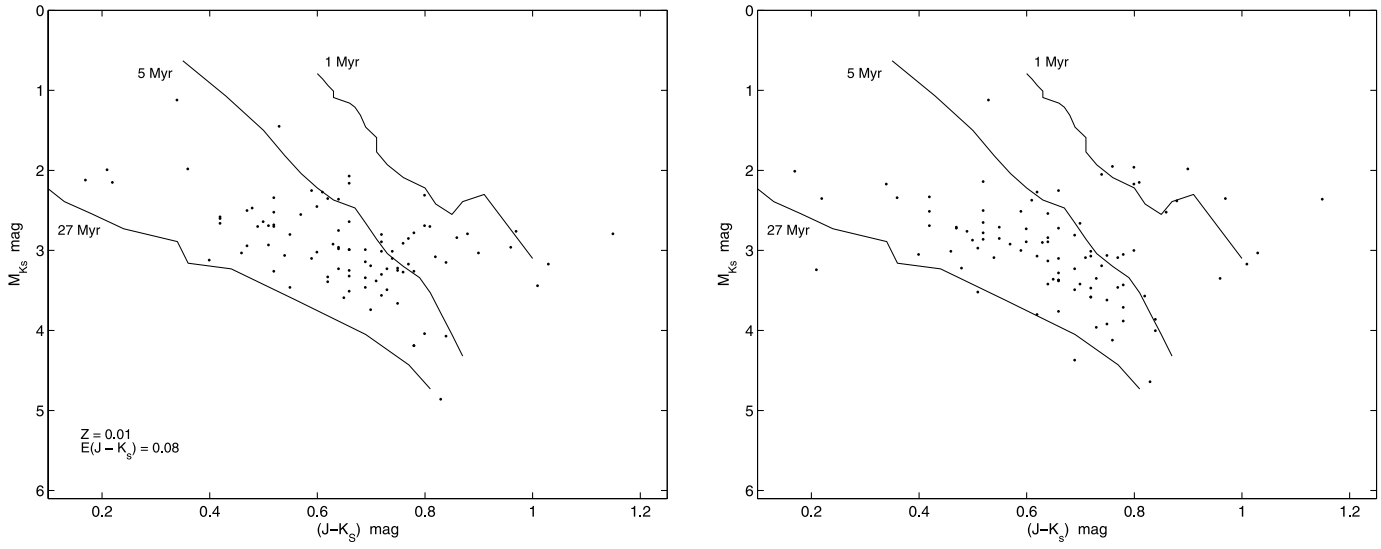


FIG. 4.—Near-infrared H-R diagrams of Lupus members, assuming the same distance of 145 pc (*left*) and with individual distances obtained by the moving-cluster method (*right*; see Table 2 and text). Three isochrones (27, 5, and 1 Myr) are drawn from Siess et al. (2000).

marked with a superscript *a* in column (1) of Table 2. Most of the other stars are confined to the area between the 5 and 27 Myr isochrones, displaying a well-outlined sequence aligned with the isochrones.

A few clues reinforce the idea that we have identified a group of stars as young as ~1 Myr in the association, which is generally older than 5 Myr. Most of these stars lie at or around the conspicuous knot at $(\alpha,\ \delta) = (242^\circ,\ -39^\circ)$, which is definitely related to the Lupus 3 dark cloud, first investigated in detail by Schwartz (1977). The emission-line CTTS members tend to crowd in this area. The Lupus 3 cloud has a filamentary structure and is quite dense (López Martí et al. 2005), although at 300 $M_\odot$ it is not the most massive cloud in the Lupus complex (Tachihara et al. 1996). The seven stars within 1° of the Lupus 3 core from the identified 1 Myr old population have markedly smaller proper motions, especially in the $\alpha \cos\delta$ component, down to $-3.7$ mas yr$^{-1}$ for RX J1609.4−3850. Unfortunately, the modest astrometric precision (at 5 mas yr$^{-1}$) for most of these stars does not allow us to establish with certainty that the youngest Lupus 3 core moves slightly differently from the greater Lupus association. Individual kinematic distances are also imprecise for this reason, but by averaging the seven estimates (Table 2), a fairly firm conclusion can be made that this nest of very young stars is located at ~170 pc from the Sun. This is about 25 pc farther than the mean distance to the greater association. One of the identified youngest stars, RX J1547.6−4018, is probably associated with the dark cloud 335.9+11.3 listed in Otrupcek et al. (2000).

## 5. CONCLUSIONS

Convergent point analysis of the proper motions of 93 high-fidelity T Tauri members of the Lupus star-forming region given in the UCAC2 catalog (Zacharias et al. 2004) reveals a kinematic group of impressive integrity, similar to that of open clusters. The internal one-dimensional velocity dispersion in the direction perpendicular to the apparent streaming motion on the sky is roughly 1.3 km s$^{-1}$. At the same time, the estimated rate of expansion is marginally significant and is too slow to account for the present-day disposition on the sky. It would have taken the association at least 30 Myr to expand into its present size at the measured rate, if it emerged from a compact star-forming region less than 30 pc diameter. A depth of ≈80 pc for the association, estimated from individual moving-cluster distances, is even larger than the extent of the surveyed area on the sky. Therefore, the Lupus association, which includes stars of diverse ages, emerged from two or more spatially separated cores.

When the individual distances estimated by the moving-cluster method are taken into account, a group of ~1 Myr old stars appears on the $M_{K_s}$ versus $J - K_s$ diagram, separated by a clear swath from the rest of Lupus stars, mostly contained between the 5 and 27 Myr isochrones. Seven of these apparently very young stars lie in the prominent concentration of mainly CTTS members associated with the Lupus 3 dark filament. Their average distance is approximately 170 pc, i.e., ≈25 pc farther than the middle of the greater Lupus association. The site of the latest star formation event is spatially segregated from the bulk of older stars.

These results appear to be a poor fit to the standard scenario of star formation, which implies the availability of stable, long-lived (≈10 Myr) hibernating molecular cores, taking their time to whittle away their magnetic field strength by ambipolar diffusion before they reach the critical density and start producing stars. The widely dispersed WTTS stars were formed close to where they are now, but there is no significant molecular gas in their neighborhood,whereas the 1 Myr old members huddle close to the prominent Lupus 3 filament and other smaller cores. It is hard to explain how a stable supercritical core of the standard model could be quickly dispersed after producing a handful of mostly K and M stars, predominant in Lupus. The emerging picture conforms to the paradigm of dynamical star formation driven by converging flows of gas and dust (Hartmann et al. 2001). A short-lived star formation episode occurs when two flows converge locally at a moderate relative velocity. Dynamical interaction of gas flows damps the velocity difference, so that the new stars formed in a short burst have similar initial velocities and slowly drift away from the site. The large extent, the complex structure, and the spread in age of the Lupus T association can be explained as the result of multiple star formation episodes at different locations and times, but within the same fragmented cloud.

The research described in this paper was carried out at the Jet Propulsion Laboratory, California Institute of Technology, under a contract with the National Aeronautics and Space Administration (NASA). This research has made use of the SIMBAD database, operated at CDS, Strasbourg, France, and data products from the 2MASS, which is a joint project of the University of Massachusetts and the Infrared Processing and Analysis Center, California Technology Institute, funded by NASA and the NSF.

## REFERENCES

Ballesteros-Paredes, J. 2006, MNRAS, 372, 443
Blaauw, A. 1964, ARA&A, 2, 213
Crawford, I. A. 2000, MNRAS, 317, 996
de Bruijne, J. H. J. 1999, MNRAS, 310, 585
de Bruijne, J. H. J., Hoogerwerf, R., & de Zeeuw, P. T. 2001, A&A, 367, 111
Dravins, D., Lindegren, L., & Madsen, S. 1999, A&A, 348, 1040
Hartmann, L., Ballesteros-Paredes, J., & Bergin, E. 2001, ApJ, 562, 852
Hughes, J., Hartigan, P., & Clampitt, L. 1993, AJ, 105, 571
James, D. J., et al. 2006, A&A, 446, 971
Krautter, J., et al. 1997, A&AS, 123, 329
López Martí, B., Eistlöffel, J., & Mundt, R. 2005, A&A, 440, 139
Makarov, V. V. 2006, AJ, 131, 2967
Makarov, V. V., Gaume, R. A., & Andrievsky, S. M. 2005, MNRAS, 362, 1109
Makarov, V. V., Olling, R. P., & Teuben, P. J. 2004, MNRAS, 352, 1199
Makarov, V. V., & Robichon, N. 2001, A&A, 368, 873
Mouschovias, T. Ch., Tassis, K., & Kunz, M. W. 2006, ApJ, 646, 1043
Otrupcek, R. E., Hartley, M., & Wang, J.-S. 2000, Publ. Astron. Soc. Australia, 17, 92
Schwartz, R. D. 1977, ApJS, 35, 161
Shu, F. H., Adams, F. C., & Lizano, S. 1987, ARA&A, 25, 23
Siess, L., Dufour, E., & Forestini, M. 2000, A&A, 358, 593
Tachihara, K., et al. 1996, PASJ, 48, 489
Wichmann, R., et al. 1997, A&A, 320, 185
Zacharias, N., et al. 2004, AJ, 127, 3043